

Spatial Coherence and the Orbital Angular Momentum of Light in Astronomy

D. Hetharia, M. P. van Exter, and W. Löffler*
*Huygens–Kamerlingh Onnes Laboratory, Leiden University,
P.O. Box 9504, 2300 RA Leiden, The Netherlands*

The orbital angular momentum (OAM) of light is potentially interesting for astronomical study of rotating objects such as black holes, but the effect of reduced spatial coherence of astronomical light sources like stars is largely unknown. In a lab-scale experiment, we find that the detected OAM spectrum depends strongly on the position of the light-twisting object along the line of sight. We develop a simple intuitive model to predict the influence of reduced spatial coherence on the propagating OAM spectrum for, e.g., astronomical observations. Further, we derive equations to predict the effect of line-of-sight misalignment and the received intensity in higher-order OAM modes for limited-size detectors such as telescopes.

The total angular momentum of paraxial light fields contains a spin (polarization) and an orbital part, where the latter is related to the azimuthal component of light’s spatial degree of freedom. For rotationally invariant intensity distributions, there are “pure” orbital angular momentum (OAM) fields that are characterized simply by a helical phase $e^{i\ell\phi}$, where ϕ is the azimuth in the chosen coordinate system, and $\ell\hbar$ is the OAM of a single photon in such a mode [1]. In general, we can characterize light via its OAM spectrum P_ℓ [2]. The OAM of light is proven to be useful in a broad range of classical and quantum optical applications, and plays a key role in vortex coronagraphy [3, 4] in astronomy, but it is an open question whether the OAM of light from deep space objects is useful for astronomical observations on earth [5–7]. There is potential, as for instance, frame-dragging of space in the vicinity of a rotating (Kerr) black hole can leave a significant trace in the OAM spectrum of the light passing through the region [8–11]. This gives potentially direct access to the spin of black holes, which is up to now only accessible via indirect methods such as relativistic line broadening by the linear Doppler shift and gravitational effects [12, 13]. We note that there are also OAM phase modifications of light passing through [14, 15] or being reflected from [16] rotating objects due to the rotational Doppler effect; but here, we study situations where the *total OAM* is modified and becomes non-zero.

Because the OAM of light is connected to the spatial degrees of freedom of light, observation thereof requires light fields with sufficient spatial (transverse) coherence [17, 18]. This is why light emission from, e.g., the black hole accretion disk itself cannot be used, instead, we consider the case of a star illuminating the black hole from behind (Fig. 1a). But also stars emit spatially incoherent light which acquires spatial coherence only upon propagation; and even if we observe starlight on earth fully coherent, it might be incoherent at the light-twisting object. The study of optical phase singularities in partially coherent fields started with the static case of a twisted

Gaussian Schell-Model beam [19, 20]. Only relatively recently, the dynamic case including propagation was investigated; this led to the discovery of circular correlation singularities [21–24], further, the precise structure of the vortices turned out to be quite different to the coherent case [25]. However, the influence of reduced spatial coherence on the experimentally accessible OAM spectrum for a light-twisting object in between is still largely unknown; mostly light without total OAM was investigated so far [23, 26]. Because the light-twisting object modifies azimuthal correlations, theoretical calculation of the propagation of the cross-spectral density function are very time consuming [23, 25]; simple models are missing for, e.g., assessment of the situation in astronomy [5, 10]. We provide here firstly such a model and confirm it by lab-scale experiments.

To set the stage we show in Fig. 1 our scheme and the lab-scale experiment emulating the source star, the light-twisting object, and the detector. We consider here the case where those objects lie approximately on a straight line, and spectrally coherent quasi-monochromatic light. Further, we work within the paraxial approximation and assume homogeneous polarization, therefore we discuss only scalar fields. Astronomical light sources are nearly always spatially completely incoherent, because of spatially uncorrelated light generation processes. To synthesize the spatially incoherent light source (star) in the lab, we image with a $10\times$ microscope objective a suitable spot from a large-area LED chip ($\lambda = 620 \pm 10$ nm) onto an aperture of diameter d_1 . During propagation to the light-twisting object (at distance L_1), a certain degree of spatial coherence is build up according to the van Cittert–Zernike theorem. The object then imprints OAM, where we use in the experiment a spiral phase plate (SPP) of charge $\Delta\ell$ [27, 28]. Finally, light propagates over distance L_2 to the observer, a OAM-spectrum analyzer. This consists of a phase-only spatial light modulator (SLM) whose surface is imaged with a $100\times$ microscope objective onto the core of a single-mode fiber (SMF) connected to a femto-watt photo detector. We modulate the LED at around 500 Hz and use lock-in detection. The SLM holograms are restricted to a circular area to select our detection aperture d_2 , which corresponds to the telescope entrance

* loeffler@physics.leidenuniv.nl

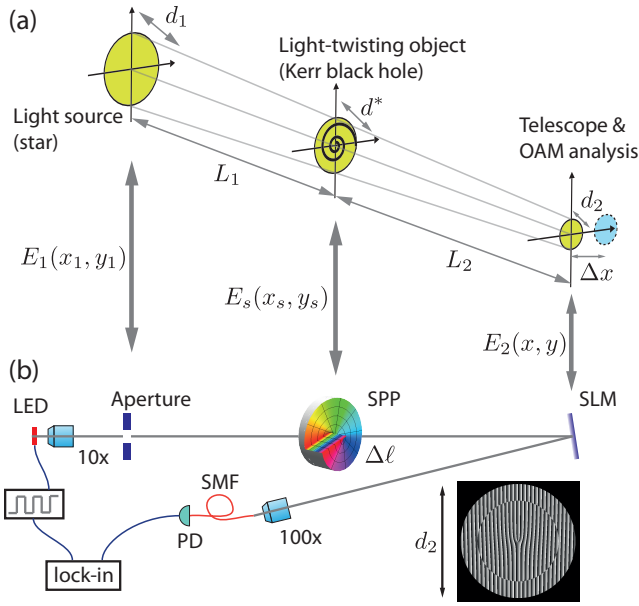


Figure 1. (a): The scheme: A spatially incoherent source of diameter d_1 such as a star illuminates a region of space that modifies the OAM of light, for instance a Kerr black hole. On earth, a telescope or interferometer with an effective diameter (baseline) of d_2 is used to measure the OAM spectrum. (b): Lab-scale experimental setup. To simulate the star, we use a spatially incoherent light source (LED) illuminating the first aperture; the spiral phase plate (SPP) with charge $\Delta\ell$ mimics the light-twisting object that modifies the OAM. A combination of phase-only spatial light modulation (SLM; see inset for an exemplary hologram) and imaging onto the core of a single-mode fiber (SMF) coupled to a photo-diode (PD) is used to measure the OAM spectrum; the aperture d_2 on the SLM corresponds to the telescope diameter.

aperture. For determination of the azimuthal-only OAM spectrum, we need to integrate over the radial coordinate, for which we sum over the lower 5 “Walsh-type” radial modes [29], which turns out to be a very reliable method; the inset in Fig. 1b shows an example hologram for $\ell = 2$. By displaying a series of vortex holograms on the SLM, we can measure the OAM spectrum P_ℓ . We assume for now perfect line of sight condition, i.e., $\Delta x \equiv 0$.

Fig. 2a and b show the OAM spectra P_ℓ for two choices of the source diameter d_1 . We recognize the approximately triangular OAM spectrum, which has been found before [30], this is due to the hard edges of the source and detector aperture, and mathematically based on the Fourier relation between a squared spherical Bessel function and the triangular function. We now introduce a SPP with $\Delta\ell = 2$ at distance L_1 from the first aperture; the resulting OAM spectra are shown in Fig. 2c and d. Contrary to naive expectation, we do *not* simply observe a spectrum that is shifted by $\Delta\ell = 2$, but we observe a deformed OAM spectrum where the average shift is smaller than $\Delta\ell = 2$. Further, we see that, the lower the spatial coherence of the source (i.e., the larger aperture d_1), the

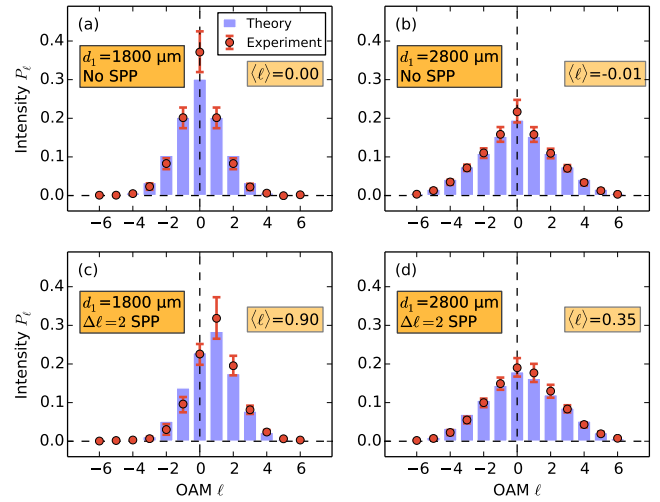


Figure 2. Measured OAM spectra (red dots, P_ℓ versus ℓ) for different aperture sizes: (a,c) $d_1 = 1800 \mu\text{m}$, (b,d) $d_1 = 2800 \mu\text{m}$. (a,b) are measured without the SPP, and (c,d) with a $\Delta\ell = 2$ SPP introduced $L_1 = 560$ mm behind the source aperture d_1 . The experimental error is estimated from multiple measurements (10%) and the uncertainty in d_1 ($\pm 50 \mu\text{m}$). The bars show the theoretical results (no fit parameters). Common parameters: $d_2 = 800 \mu\text{m}$, $L_2 = 315$ mm.

smaller the average OAM $\langle \ell \rangle = \sum_\ell \ell P_\ell$. Note that if we use a single-mode source (not shown), we observe a shift of $\Delta\ell = 2$, as expected.

How can this be understood? Let us consider briefly two extreme cases: Clearly, if we place the SPP very close to the spatially incoherent source (regime A), its action vanishes: The OAM spectrum of the source is at the SPP position very broad compared to the small $\Delta\ell$ of the SPP, but the detector will receive only a narrow spectrum around $\ell = 0$. Consequently, it detects a nearly unshifted OAM spectrum. Equally obvious is the opposite extreme regime (B), if the SPP is placed very close to the detector, it will then detect a $\Delta\ell$ -shifted OAM spectrum, since the action of the SPP can be added to the holograms used for measurement of the OAM spectrum. Useful cases in astronomy must lie in between those regimes: Regime A is irrelevant since OAM carries no additional information, and case B is unrealistic as extremely close black holes are highly unlikely.

To study the general case, we develop a theory and an intuitive model that explains our experimentally observed OAM spectrum for arbitrary aperture sizes, positions of the SPP, and SPP charges $\Delta\ell$. We could simply calculate the cross-spectral density function W at the detector, and determine from it the OAM spectrum, but this gives little insight and is very time-consuming. In particular because we also want to study the case where the observer is not exactly on the line-of-sight ($\Delta x \neq 0$) and no symmetries can be exploited for simplification [23]. Our approach here is to model the incoherent source by a number of

Huygens elementary sources at (x_1, y_1) , each illuminating the SPP with a spherical wave (which is conceptually related to the method used in [22]). For the field directly behind the SPP we obtain ($k = 2\pi/\lambda$):

$$E_s(x_s, y_s) = \frac{\exp[ikR_s]}{R_s} \cdot \exp(i\Delta\ell\phi) \quad (1)$$

with $R_s^2 = (x_s - x_1)^2 + (y_s - y_1)^2 + L_1^2$

We then propagate this field to the detector (E_2) numerically, using the well-known Huygens-Fresnel principle:

$$E_2(x, y) = \int dx_s dy_s E_s(x_s, y_s) \exp(i\frac{2\pi}{\lambda}R)/R \quad (2)$$

with $R^2 = (x - x_s)^2 + (y - y_s)^2 + L_2^2$

For each elementary source at (x_1, y_1) , the OAM spectrum $P_\ell(x_1, y_1) = \int_0^{d_1/2} r dr |\int d\phi E_2(r, \phi) \exp(i\ell\phi)|^2$ is calculated and summed up incoherently for all sources: $P_\ell = \int dx_1 dy_1 E_1(x_1, y_1) P_\ell(x_1, y_1)$. In case $\Delta x = 0$ (exactly in line-of-sight), due to symmetry, we can avoid one integral and only propagate Huygens sources emerging from along a radius of the source (e.g., for $0 < x_1 < d_1/2$ with $y_1 = 0$), and add a radial factor in summing up the OAM spectra as $P_\ell = \int_0^{d_1/2} dx_1 x_1 P_\ell(x_1, y_1 = 0)$. The result of this numerical simulation is compared in Fig. 2 to the experimental data; we see good agreement and good reproduction of the OAM spectrum deformations.

But for applications of OAM, the precise shape of the spectrum is often not relevant. Hence, we focus in the following on the *mean OAM* $\langle \ell \rangle$, which is directly measurable experimentally [31]. We find here that the mean OAM is a robust quantity that allows further approximations of Eq. 2 [32] and also to derive a simple model.

First, we investigate the dependency of the OAM mean $\langle \ell \rangle$ on the diameter of the source d_1 . In an astrophysical context this corresponds to the diameter of the source star, which determines the degree of spatial coherence at the position of the light-twisting object. In Fig. 3 we compare d_1 -dependent experimental data with the theory (Eq. 2). We see that only for very small source diameter, the full OAM shift introduced by the SPP is also detectable at the detector. We have measured this for two spiral phase plates with $\Delta\ell = 1, 2$ in Fig. 3, the similar shape of the curves suggests that the charge of the SPP is simply a scaling parameter, at least for low $\Delta\ell$, we therefore normalize in the following the observed mean OAM by $\Delta\ell$.

How can we estimate the detected mean OAM in terms of a simple model? We found that we simply have to compare the coherence length $L_i^c = 1.22\lambda L_i/d_i$ of the source star L_1^c and that of the backpropagated detector L_2^c at the position of the light-twisting object as follows:

$$\mathcal{F} = \frac{L_1^c}{L_1^c + L_2^c} = \frac{d_2 L_1}{d_2 L_1 + d_1 L_2}, \quad (3)$$

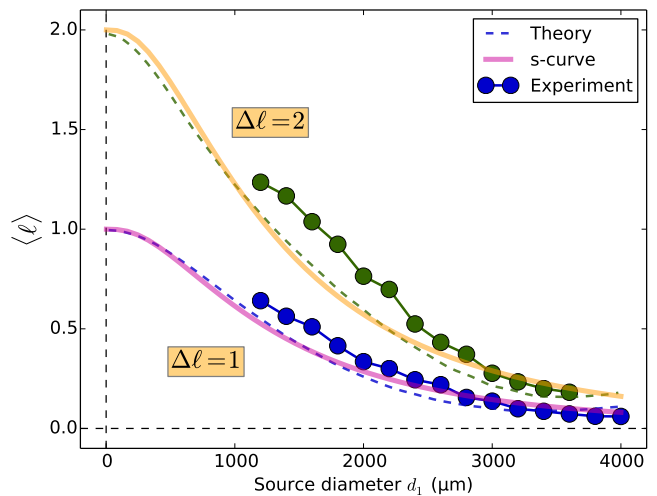


Figure 3. The detected mean OAM as a function of the aperture size d_1 for $\Delta\ell = 1$ and $\Delta\ell = 2$ spiral phase plates placed $L_1 = 56$ cm behind the first aperture ($d_2 = 800 \mu\text{m}$, $L_2 = 315$ mm). The experimental data (symbols) agree well to the theory (Eq. 2) and the simple s-curve model.

To confirm this choice, Fig. 4 shows the previous d_1 -dependent calculation together with new L_1 -dependent calculations. We find that the data points lie on a common curve. This confirms that all distance (L_1, L_2), diameter (d_1, d_2), and SPP charge ($\Delta\ell$) dependencies can nicely be mapped by \mathcal{F} onto a sigmoid-shaped curve. A s-shaped curve that fits best and has fewest parameters is the incomplete Beta function, we obtain for the mean OAM $\langle \ell \rangle = \Delta\ell \cdot B(\mathcal{F}, 3.5, 3.1)$, see Fig. 4. This agrees perfectly with the intuitive picture that we have presented in the beginning, namely that if the SPP is close to the source ($L_1 \ll L_2$, assuming $d_1 \approx d_2$), its action disappears because the field at that position is highly incoherent. On the other hand, very close to the detector ($L_1 \gg L_2$), the OAM shift $\Delta\ell$ from the SPP is fully reflected in the detected mean of the OAM spectrum $\langle \ell \rangle$, independent of the spatial coherence of the field there. An estimation of the fidelity parameter Eq. 3 could also be derived from relating the detector diameter d_2 to the coherence singularity diameter $d_2^c = d_1 L_2 / L_1$ at the position of the detector [22]. This explains why the expression 3 is not wavelength dependent: for longer wavelengths, diffraction only reduces the overall intensity and does not modify the ratio between the individual detected OAM modes.

Now, we discuss the possibility of using light's OAM in astronomical observations of massive, space-distorting objects such as rotating black holes that might twist light [9, 10]. As an example, we consider the supermassive Kerr black hole at the center of our galaxy, Sagittarius A* (Sgr A*) with a Schwarzschild radius of $R_s = 1.27 \times 10^{12}$ m, where it is reasonable to assume that all light that we receive is modified [10]. First, is observation at radio frequencies or with visible light

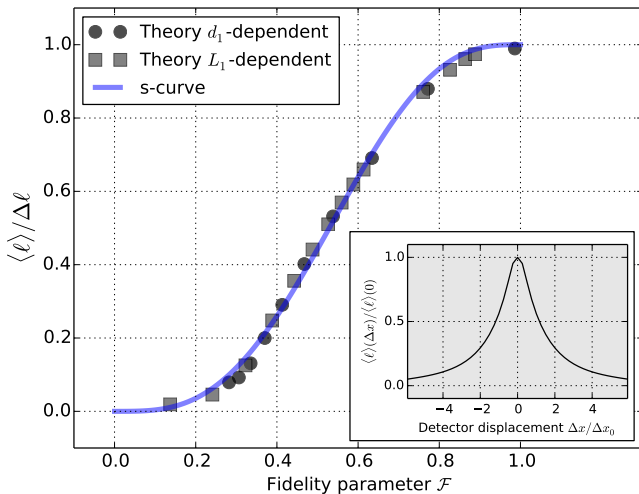


Figure 4. Detected normalized mean OAM for d_1 and L_1 dependent calculation (symbols), plotted as a function of the parameter \mathcal{F} . Both calculations lie on a s-shaped curve that is nicely represented by the incomplete Beta-function (curve). Inset: Calculated mean OAM as a function of detector displacement in multiples of $\Delta x_0 = \sqrt{d_1 d_2 L_2 / L_1}$, relative to the exact line-of-sight condition $\Delta x = 0$.

advantageous? Although the wavelength λ disappeared from Eq. 3, it affects the overall detected intensity (which scales as $[d_2^2 / (L_2 / k)]^{|\Delta \ell|}$, see below). In these terms, most radio telescope arrays are comparable to visible-light interferometric telescopes, we select as an example the next-generation Magdalena Ridge Observatory Interferometer (MROI) with $d_2 = 340$ m baseline, operating at $\lambda = 600$ nm with an angular resolution of 1.8×10^{-9} rad. This telescope would receive from this area [at $L_2 = 25.9 \times 10^3$ light years (ly) distance] up to $N_{OAM} = 2.3$ optical OAM modes [30]. However, as we have shown, it is highly unlikely that such a large area will be illuminated spatially coherently. It is more realistic to assume that a sun-like star or pulsar is illuminating Sgr A* from behind, exactly on the line of sight, we choose $d_1 = 1.4 \times 10^9$ m. From Eq. 3 we see that, to observe on earth a mean OAM $\langle \ell \rangle = \Delta \ell / 2$ (i.e., 50% shift), we have the extreme requirement that distance $L_1 > d_1 L_2 / d_2 \approx 10^{11}$ ly, which is impossible. However, more recent studies suggest that a large number of smaller black holes exist in every galaxy such as ours; for instance, for a black hole in the Orion nebula at $L_2 = 1500$ ly distance [33], an illuminating object at only $L_1 = 6 \cdot 10^9$ ly would be needed. If we can detect a 1% OAM shift $\langle \ell \rangle = 0.01 \cdot \Delta \ell$, an illuminating star at $L_1 = 6 \cdot 10^7$ ly would suffice.

Up to now, the source, the light-twisting object, and the observer were considered to be perfectly on a line. For large detectors, it is known that misalignment leaves the mean OAM unchanged, only the variance of the OAM spectrum increases [34–37]. Here, however, due to the limited aperture of our detector, we find that the de-

tected mean OAM $\langle \ell \rangle$ is reduced by transverse misalignment Δx , calculated by modifying $P_\ell(x_1, y_1)$ below Eq. 2. For a coherent light source, if the detector is displaced by more than its diameter, i.e., $\Delta x \gg d_2$, the detected mean OAM $\langle \ell \rangle(\Delta x)$ vanishes. This would render OAM useless for astronomy because of typically very large transverse speeds, e.g., the earth is moving at $v = 30$ km s $^{-1}$ around the sun. However, for partially coherent light, we find a different scaling parameter $\Delta x_0 = \sqrt{d_1 d_2 L_2 / L_1}$, see the inset in Fig. 4, where the calculated mean OAM normalized to zero displacement $\langle \ell \rangle(\Delta x) / \langle \ell \rangle(\Delta x = 0)$ is shown. For the case of a rotating black hole in the Orion nebula (see above, for 1% OAM shift), we obtain $\Delta x_0 = 3450$ m, much larger than the detector size; reduced spatial coherence is actually advantageous here. The observation of $\langle \ell \rangle$ -transients due to relative motion opens up a novel possibility to find, for instance, close-by black holes as generally, non-zero total OAM is expected to be strictly absent.

Finally, we briefly discuss a well-known but often ignored fact: During propagation from the light-twisting object (SPP) to the detector, the vortex core expands due to diffraction, and if its effective diameter is large compared to the detector, the detected intensity is much lower compared to the case without SPP. In the astronomy case, the earth-bound observer is certainly always in this regime and for estimation of this effect, we find that the size of the dark core of an OAM mode scales as $(1 + \ell/2) \sqrt{L_2 / k}$ (in agreement with the $\ell = 1$ case in [27]). The integrated intensity captured by a detector of diameter d_2 is [38], relative to the plane-wave case, $I_{det}(\ell) / I_{det}(0) = \pi (d_2^2 k / 4z)^{|\ell|} / (1 + |\ell|)$. For the case of Sgr A* observed with the MROI, this ratio is approximately $10^{-9|\ell|}$, suggesting that OAM is only suitable for observation of much closer light-twisting objects, because an OAM astronomer sits always in the “shadow of the phase singularity”. But mind that this is always the case if we can resolve an image of an object far away.

In conclusion, we have found experimentally and theoretically that insertion of a light-twisting object, such as a spiral phase plate with charge $\Delta \ell$, in light with reduced spatial coherence results in detected OAM spectra which depend strongly on the position of this object. This contrasts with the well-known coherent case, where simply a displacement of the OAM spectrum by $\Delta \ell$ occurs. We have derived a simple parameter (Eq. 3) for the mean of the detected OAM spectrum $\langle \ell \rangle$ as this is key for applications. For observation of a nonzero OAM shift, it is required that as few as possible modes from the source illuminate the light-twisting object, and as many modes as possible are detected from it by the observer. With this, we have assessed the use of OAM in astronomy and find that with current technology, only close-by light-twisting objects are within reach; additionally, low light levels and line-of-sight mismatch must be taken into account seriously. However, the detrimental effects of line-of-sight misalignment might be smaller for spatially incoherent

sources, thus first detection of astronomical OAM could actually be facilitated in this case. It would be interesting to study the influence of gravitational (micro-) lensing [39], possibly by the black hole itself [40], on light collection and the line-of-sight criterion; wave-optical studies

of these cases are needed.

ACKNOWLEDGMENTS

We acknowledge Christoph Keller (Leiden) for fruitful discussions and financial support by NWO (grant number 680-47-411).

-
- [1] L. Allen, M. W. Beijersbergen, R. J. C. Spreeuw, and J. P. Woerdman, *Phys. Rev. A* **45**, 8185 (1992).
 - [2] G. Molina-Terriza, J. P. Torres, and L. Torner, *Phys. Rev. Lett.* **88**, 013601 (2001).
 - [3] G. Foo, D. M. Palacios, and G. A. Swartzlander, Jr., *Opt. Lett.* **30**, 3308 (2005).
 - [4] D. Mawet, P. Riaud, O. Absil, and J. Surdej, *Astrophys. J.* **633**, 1191 (2005).
 - [5] M. Harwit, *Astrophys. J.* **597**, 1266 (2003).
 - [6] G. C. G. Berkhout and M. W. Beijersbergen, *Phys. Rev. Lett.* **101**, 100801 (2008).
 - [7] G. C. G. Berkhout and M. W. Beijersbergen, *J. Opt. A* **11**, 094021 (2009).
 - [8] P. Carini, L. L. Feng, M. Li, and R. Ruffini, *Phys. Rev. D* **46**, 5407 (1992).
 - [9] L.-L. Feng and W. Lee, *Int. J. Mod. Phys. B* **10**, 961 (2001).
 - [10] F. Tamburini, B. Thide, G. Molina-Terriza, and G. Anzolin, *Nat. Phys.* **7**, 195 (2011).
 - [11] H. Yang and M. Casals, *Phys. Rev. D* **90**, 023014 (2014).
 - [12] A. C. Fabian, K. Iwasawa, C. S. Reynolds, and A. J. Young, *Publ. Astron. Soc. Pac.* **112**, 1145 (2000).
 - [13] G. Risaliti, F. A. Harrison, K. K. Madsen, D. J. Walton, S. E. Boggs, F. E. Christensen, W. W. Craig, B. W. Grefenstette, C. J. Hailey, E. Nardini, D. Stern, and W. W. Zhang, *Nature* **494**, 449 (2013).
 - [14] J. B. Götte, S. M. Barnett, and M. Padgett, *Proc. R. Soc. A* **463**, 2185 (2007).
 - [15] J. Leach, A. J. Wright, J. B. Götte, J. M. Girkin, L. Allen, S. Franke-Arnold, S. M. Barnett, and M. J. Padgett, *Phys. Rev. Lett.* **100**, 153902 (2008).
 - [16] M. P. J. Lavery, F. C. Speirits, S. M. Barnett, and M. J. Padgett, *Science* **341**, 537 (2013).
 - [17] L. Mandel and E. Wolf, *Optical Coherence and Quantum Optics* (Cambridge University Press, 1995).
 - [18] M. Born and E. Wolf, *Principles of Optics: Electromagnetic Theory of Propagation, Interference and Diffraction of Light* (Cambridge University Press, 1999).
 - [19] R. Simon and N. Mukunda, *J. Opt. Soc. Am. A* **10**, 95 (1993).
 - [20] J. Serna and J. M. Movilla, *Opt. Lett.* **26**, 405 (2001).
 - [21] I. D. Maleev, D. M. Palacios, A. S. Marathay, and J. Grover A. Swartzlander, *J. Opt. Soc. Am. B* **21**, 1895 (2004).
 - [22] D. M. Palacios, I. D. Maleev, A. S. Marathay, and G. A. Swartzlander, *Phys. Rev. Lett.* **92**, 143905 (2004).
 - [23] H. D. L. Pires, J. Woudenberg, and M. P. van Exter, *J. Opt. Soc. Am. A* **27**, 2630 (2010).
 - [24] Y. Yang, M. Chen, M. Mazilu, A. Mourka, Y.-D. Liu, and K. Dholakia, *New J. Phys.* **15**, 113053 (2013).
 - [25] G. A. Swartzlander and R. I. Hernandez-Aranda, *Phys. Rev. Lett.* **99**, 163901 (2007).
 - [26] M. Malik, S. Murugkar, J. Leach, and R. W. Boyd, *Phys. Rev. A* **86**, 063806 (2012).
 - [27] S. Khonina, V. Kotlyar, M. Shinkaryev, V. Soifer, and G. Uspleniev, *J. Mod. Opt.* **39**, 1147 (1992).
 - [28] M. W. Beijersbergen, R. P. C. Coerwinkel, M. Kristensen, and J. P. Woerdman, *Opt. Commun.* **112**, 321 (1994).
 - [29] D. Geelen and W. Löffler, *Opt. Lett.* **38**, 4108 (2013).
 - [30] H. D. L. Pires, J. Woudenberg, and M. P. van Exter, *Opt. Lett.* **35**, 889 (2010).
 - [31] B. Piccirillo, S. Slussarenko, L. Marrucci, and E. Santamato, *arXiv* **1305.1496** (2013), arXiv:1305.1496.
 - [32] In the intermediate regime, we found that the Fresnel propagator can be completely removed without strongly modifying (ℓ).
 - [33] L. Šubr, P. Kroupa, and H. Baumgardt, *Astrophys. J.* **757**, 37 (2012).
 - [34] G. Gibson, J. Courtial, M. Padgett, M. Vasnetsov, V. Pas'ko, S. Barnett, and S. Franke-Arnold, *Opt. Express* **12**, 5448 (2004).
 - [35] M. V. Vasnetsov, V. A. Pas'ko, and M. S. Soskin, *New J. Phys.* **7**, 46 (2005).
 - [36] R. Zambrini and S. M. Barnett, *Phys. Rev. Lett.* **96**, 113901 (2006).
 - [37] W. Löffler, A. Aiello, and J. P. Woerdman, *Phys. Rev. Lett.* **109**, 113602 (2012).
 - [38] This is calculated based on the $\sim r^{|\ell|}$ amplitude close to the vortex core and confirmed via numerical simulations. Mind that this is different for exact Laguerre-Gaussian beams.
 - [39] I. Ciufolini and F. Ricci, *Classical Quant. Grav.* **19**, 3863 (2002).
 - [40] V. Bozza, *Gen. Relat. Gravit.* **42**, 2269 (2010).